

Reflection and transmission coefficients of self-similar interfaces

Kees Wapenaar
Delft University of Technology
Centre for Technical Geoscience
Lab. of Seismics and Acoustics, P.O. Box 5046, 2600 GA Delft,
The Netherlands

March 9, 1998

Introduction. Reflection and transmission coefficients are generally derived for discrete interfaces between homogeneous layers, meaning that $c(z)$ and $\varrho(z)$ are assumed to behave as step-functions. Outliers in well-logs are generally quite different from step-functions. Hence, it makes sense to consider other parameterizations of $c(z)$ and $\varrho(z)$ around an interface. We present reflection and transmission coefficients of interfaces that are parameterized by self-similar singularities and we analyze the reflection and transmission responses of such an interface and of its smoothed version.

Exact reflection and transmission coefficients. We parameterize the velocity $c(z)$ around an interface at $z = 0$ as

$$c(z) = \begin{cases} c_1 |z/z_1|^{\alpha_1} & \text{for } z < 0 \\ c_2 |z/z_2|^{\alpha_2} & \text{for } z > 0, \end{cases} \quad \text{with } \alpha_1, \alpha_2 \leq \frac{1}{2}. \quad (1)$$

For a two-sided singularity (Figure 1a), with $\alpha_1 = \alpha_2 = \alpha$, this function is self-similar, according to $c(\beta z) = \beta^\alpha c(z)$; its normal incidence reflection and transmission coefficients read (for positive ω)

$$R = j \left[\frac{e^{-j\nu\pi} \varrho_2 c_2^{2\nu} + e^{j\nu\pi} \varrho_1 c_1^{2\nu}}{\varrho_2 c_2^{2\nu} + \varrho_1 c_1^{2\nu}} \right] \quad \text{and} \quad T = 2 \sin(\nu\pi) \left[\frac{\sqrt{\varrho_2 c_2^{2\nu} \varrho_1 c_1^{2\nu}}}{\varrho_2 c_2^{2\nu} + \varrho_1 c_1^{2\nu}} \right], \quad (2)$$

with $\nu = \frac{1}{2-2\alpha}$. Both coefficients are frequency-independent. The phase of R is largely determined by the factor j , which corresponds to a Hilbert transformation in the time domain. The transmission coefficient has zero phase. The reflection and transmission responses at $z_1 = -5\text{m}$ and $z_2 = 5\text{m}$ are represented by the dashed lines in Figure 2.

For a single-sided singularity (Figure 1b), with $\alpha_1 = 0$ and $\alpha_2 = \alpha$, the reflection and transmission coefficients read

$$R = \left(\frac{\frac{\Gamma(\nu)}{\Gamma(1-\nu)} (j\omega\nu|z_2|)^{1-2\nu} \varrho_2 c_2^{2\nu} - \varrho_1 c_1}{\frac{\Gamma(\nu)}{\Gamma(1-\nu)} (j\omega\nu|z_2|)^{1-2\nu} \varrho_2 c_2^{2\nu} + \varrho_1 c_1} \right) \quad \text{and} \quad T = \left(\frac{\frac{2\sqrt{\pi}}{\Gamma(1-\nu)} \sqrt{(j\omega\nu|z_2|)^{1-2\nu} \varrho_2 c_2^{2\nu} \varrho_1 c_1}}{\frac{\Gamma(\nu)}{\Gamma(1-\nu)} (j\omega\nu|z_2|)^{1-2\nu} \varrho_2 c_2^{2\nu} + \varrho_1 c_1} \right). \quad (3)$$

Both coefficients are frequency-dependent. The factor $(j\omega)^{1-2\nu}$ corresponds to a fractional differentiation/integration. For $\nu = \frac{1}{2}$ (i.e., $\alpha_1 = \alpha_2 = 0$) equations (2) and (3) both lead to the usual (flux-normalized) coefficients.

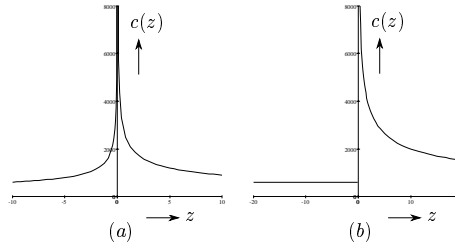


Figure 1: (a) Two-sided singularity ($\alpha_1 = \alpha_2 = \alpha = -0.4$). (b) One-sided singularity ($\alpha_1 = 0, \alpha_2 = \alpha = -0.4$).

An embedded singularity. Figure 3 shows a multiscale analysis of the two-sided singularity of Figure 1a (Mallat and Hwang, 1992, IEEE Trans. Inform. Theory, **38**, no. 2, 617-643; Herrmann, 1997, Ph.D. thesis, Delft Univ. of Techn.). The slope of the amplitude-versus-scale (AVS) curve in Figure 3d corresponds to the singularity exponent $\alpha = -0.4$. Figure 4d shows a similar AVS curve for a singularity, embedded between two homogeneous half-spaces. For small scales σ we observe $\alpha \rightarrow -0.4$, as in Figure 3d. Hence, in the high-frequency range we expect a similar response as without the embedding half-spaces. The solid lines in Figure 2 represent the exact reflection and transmission responses of this embedded singularity. Apparently the embedding has not much effect on these responses.

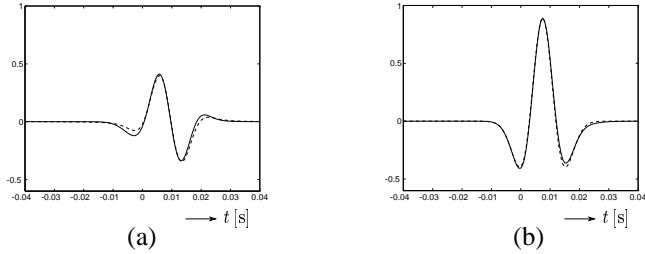


Figure 2: (a) Reflection response of the two-sided singularity of Figure 1a (dashed) and of the embedded singularity of Figure 4a (solid). The source of the incident field is a Ricker wavelet with $f_c = 50$ Hz. (b) Transmission response.

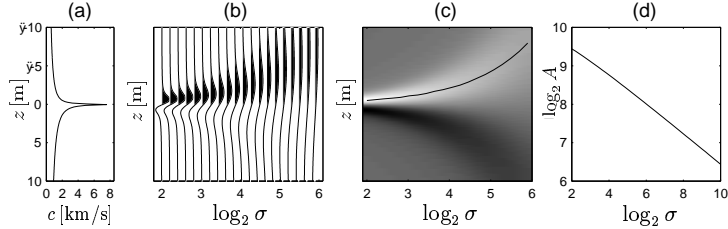


Figure 3: Multiscale analysis of a two-sided singularity (after Mallat and Hwang, 1992; Herrmann, 1997; with thanks to Jeroen Goudswaard). (a) The velocity function. (b) Continuous wavelet transform of a). (c) Modulus maxima line, obtained from b). (d) Amplitude-versus-scale (AVS) curve, measured along the modulus maxima line in c).

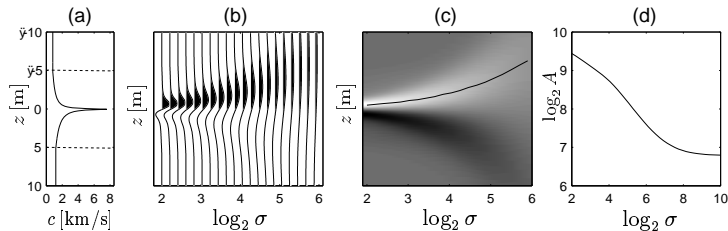


Figure 4: Multiscale analysis of a two-sided singularity, embedded between two homogeneous half-spaces.

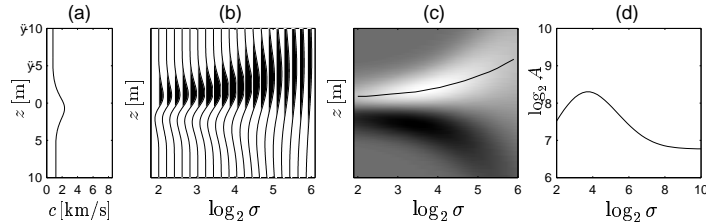


Figure 5: Multiscale analysis of a smoothed version of the embedded singularity in Figure 4a.

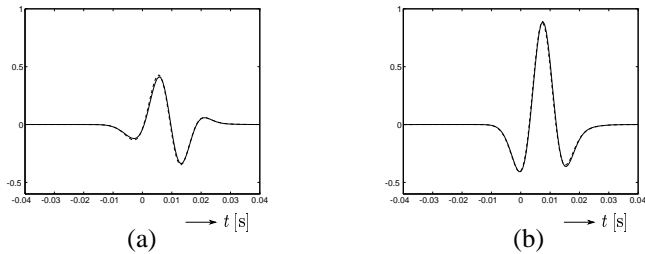


Figure 6: (a) Reflection response of the embedded two-sided singularity of Figure 4a (solid) and of its smoothed version in Figure 5a (dashed). (b) Transmission response.

A smoothed singularity. Figure 5d shows an AVS curve of a smoothed embedded singularity. In the mid-scale range the slope is equal to that of the embedded singularity (compare with Figure 4d). The reflection as well as the transmission responses are not much influenced by the smoothing (Figure 6).

Conclusions. Exact reflection and transmission coefficients for a self-similar singularity have been presented. The *band-limited* reflection and transmission responses of a self-similar singularity are reasonably stable with respect to its embedding (a large scale effect) and with respect to smoothing (a small scale effect).